

The new wave-ring helical (WRH) slow-wave structure for traveling wave tube amplifiers

Nasser Panahi¹ · S. Saviz¹ · M. Ghorannevis¹

Received: 3 April 2017 / Accepted: 13 September 2017 / Published online: 26 September 2017
© The Author(s) 2017. This article is an open access publication

Abstract In this paper, the new slow-wave structure called wave-ring helix to enhance the power of the traveling wave tubes is introduced. In this new structure, without increasing the length and radius of the helix, the wave motion path can be increased to radiofrequency wave in phase with the electron beam. The results show that in the special frequency range the output power and gain are greater than conventional helix. In this paper, optimization results are presented in cold and hot tests on the new structure. The software CST is used in S-band frequency range.

Keywords Slow-wave structure (SWS) · Traveling wave tube (TWT) · Amplifier · PIC simulation

Introduction

Helix traveling wave tube (TWT) is a microwave amplifier, which is based on the interaction of the electron beam with RF wave. The electron beam is modulated by a radiofrequency (RF) wave, and a new distribution of the electrons inside the bunch is formed. In the new distribution, RF waves received electron kinetic energy, which leads to the strengthening of the wave. In the each round of the helix, RF waves are amplified [1].

A TWT consists of an electron source, a magnetic focusing system, input and output ports of RF wave, slow-wave structure and collector. The slow-wave structure is held by three bars. TWT system is placed in a metal enclosure or ceramic [2]. The proper functioning of TWT depends on the precise balance of dielectric material and metal as well as cleaning of surfaces. In the past, several slow-wave structures to control the RF wave velocity in the form of a helix [3], contrawound helical [4], and ring-bar [5], ring-loop [6], and folded waveguide [7] and half-ring helical [8] are presented and introduced.

The ring-bar circuit, for the high-power performance of a helix type circuit is developed. In fact, ring-bar circuit is derived from the contrawound helical. In this regard, in this article instead of the simple ring, the wave-ring is used (Fig. 1). The main advantages of this type of circuit are discontinuation of the return waves (BWO) and taking advantage of its higher voltage than the single helix [9] (Fig. 2). With the discontinuation of BWO, the inside of helix space is filled with a dense electron beam; therefore, a larger beam with a high current is used. The weakness of our new helix is that the bandwidth is less than a single helix [10].

The WRH circuit design is more complex than a spiral one because the phase velocity is controlled by the thickness and length of the rod and ring. The phase and group velocities are reduced by adding the dielectric material as the holder into the inside of the helix. On the other hand, the addition of metal leads to increment of the dispersion [11, 12].

In this paper, a three-dimensional model of the WRH is simulated using the CST software. Initially, all the parts are designed using three-dimensional PIC CST software modules. Then hot test analysis is performed. The following parameters are analyzed in this three-dimensional

✉ S. Saviz
Shahrooz.saviz@srbiau.ac.ir

¹ Plasma Physics Research Center, Science and Research Branch, Islamic Azad University, Tehran, Iran

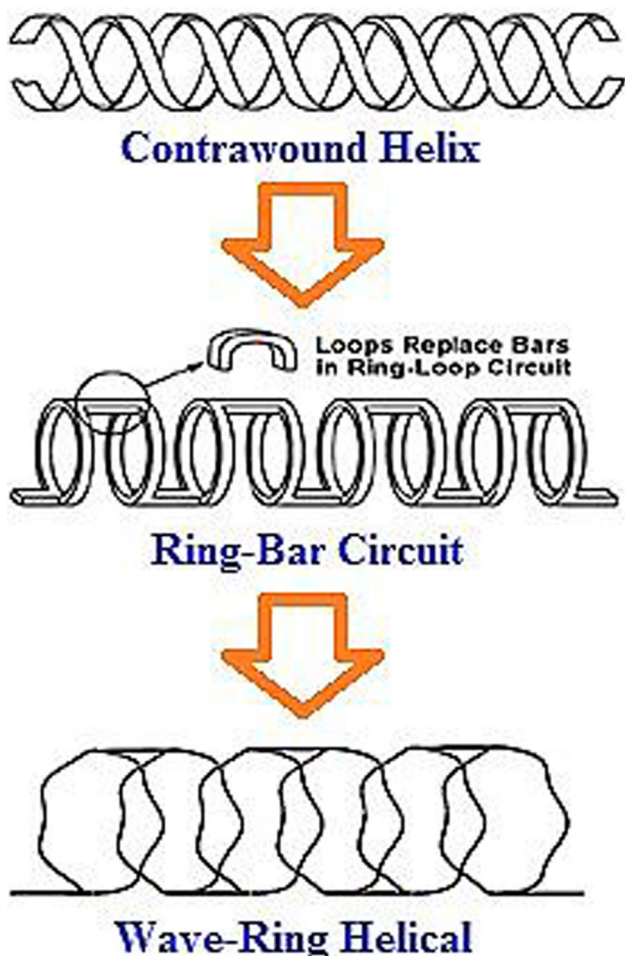


Fig. 1 Helix structure of the new and the previous structure

model: the phase velocity, circuit impedance matching, the electric field and helix circuit interaction with the electron beam.

Design of the slow-wave structure

The phase velocity and wavelength of light are reduced in the slow-wave structure tube. In this work, the bandwidth of TWT is about 2 GHz. In this area, significant improvements are observed in output power and efficiency. The WRH is constructed by combining bars and wave-ring, which results in reducing the size of the tube and eventually the phase velocity.

The perimeter of the helix is about 36.2781 mm (Fig. 3). Figure 4 represents a helix structure for traveling wave tube. Inside the helix, the wave phase velocity decreases by L .

$$v_p \cong c \sin \varphi \rightarrow \frac{v_p}{c} \cong \frac{L}{\sqrt{(2\pi a)^2 + L^2}}$$

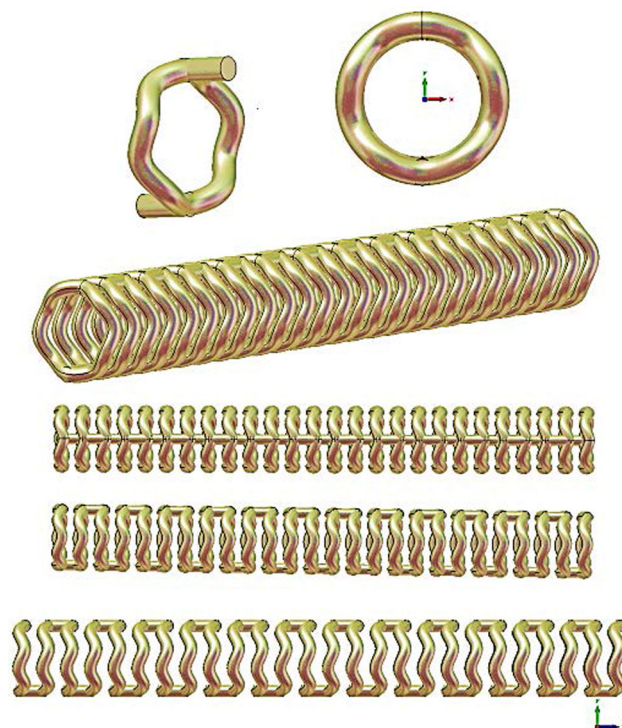


Fig. 2 Wave-ring helical circuit from different angles

The phase velocity v_p is constant and independent of frequency. Thus, the energy coupling at all frequencies occurred when the electron beam velocity is close to the phase velocity of light. The dispersion relations are obtained by applying the appropriate boundary conditions [13–15]. The parameters of the WRH are presented in Table 1.

As seen in Fig. 5, the three ventilated dielectric surrounding the helix are used to reduce heat loss and increase the bandwidth of the tube. The bars in structure are used to increase the output power and prevent the oscillations in the return wave [16]. The demands of the today’s traveling wave tubes are the high values of the output power and wide bandwidth. The embedded grooves are used to put the helix on the holder.

In this paper, our aim is to reduce the losses by selecting the appropriate structures, increase the contact area of helix with rod holder and using aluminum nitride (loss free) with permittivity coefficient of 8.6. The optimal values of these parameters are shown in Table 2.

In Fig. 6, the cavity of the WRH structure that is illustrated is of a perfect electric conductor (PEC).

The short length of TWT is a limiting factor at low frequencies. In this paper, the WRH is used to overcome this limitation. So without increasing the length of the coil, its environment can be increased which leads to a further reduction of phase velocity than the conventional helix. At

Fig. 3 Wave-ring helical circuit dimensions based on parametric equation $x = 5.5\sin(t)$, $y = 5.5\cos(t)$ and $z = 0.5\cos(5t)$ that are drawn in CST

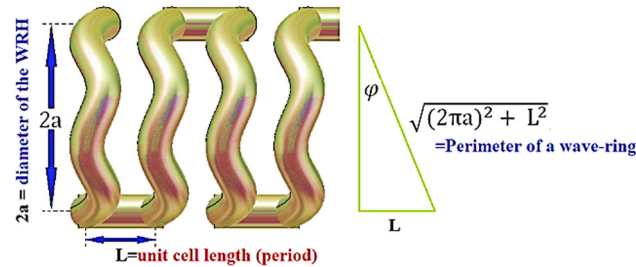
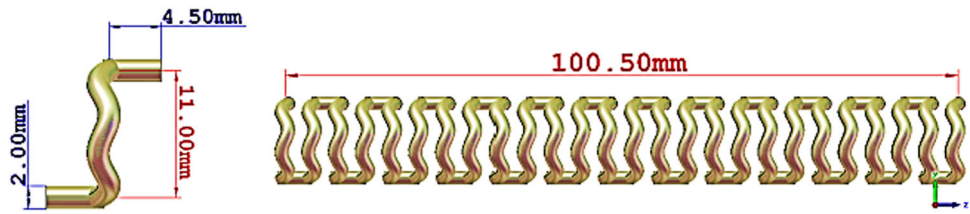


Fig. 4 Parameters in the wave-ring helical circuit

Table 1 Parameters used in the WRH structure

Parameters	Values
The thickness of the transmission line	2.00 mm
Thick metal box body	1.00 mm
The distance between the ring or rings	4.50 mm
The radius of the ring (a)	5.50 mm
Number of rings	26
Cavity radius	8.50 mm
Cavity length	140.00 mm
Holder width	3.00 mm

Table 2 The characteristics of rods

Characteristic	Description/value
Material	Aluminum nitride (loss free)
Type	Normal
Epsilon	8.6
Mue	1
Rho	3260 (kg/m ³)
Therm. cond.	200 (W/K/m)
Heat cap.	0.74 (kJ/K/kg)
Diffusivity	8.2905e-005 (m ² /s)
Young's mod.	308 (kN/mm ²)
Poiss. ratio	0.22
Thermal exp.	3.9 (1e-6/K)

that is perfect electric conductor (PEC).



Fig. 6 The cavity surrounding of SWS

$$C = K^{1/3} \left(\frac{eI}{4\gamma^3 m v_e^2} \right)^{1/3}, K(\omega) = \frac{E_{axial}^2}{2\beta^2 P},$$

where I is the electron beam current, β propagation constant of the RF wave, K interaction impedance of the SWS for one period, γ electron beam relativistic parameter, m electron mass, e electron charge, v_e electron velocity, E_{axial} peak axial electric field at the center, P total RF power flow in the structure, and $N = L/\lambda_g$ is the number of guided wavelengths along the chosen TWT of length L .

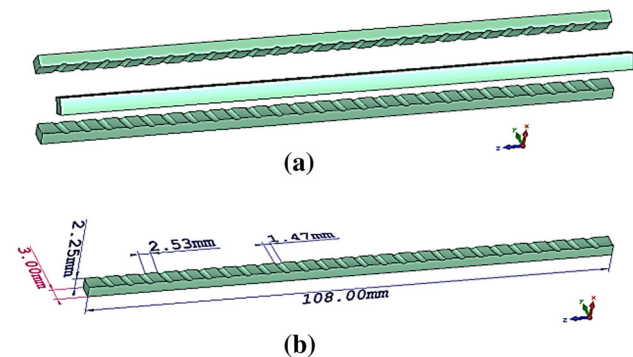


Fig. 5 **a** The simulated new structure with three rods, **b** scale of the rod is used in the structure

high frequencies, the amplified RF wave leads to further acceleration of the electron beam and lowest dispersion. Phase velocity must be constant throughout the helix. The gain is expressed by the following equation [17]:

$$G = -9.54 + 47.3CN(\text{dB}),$$

in which

Analysis and process simulation

Cold test simulation results

The special modes of periodic structure are calculated to test the structure of WRH. For this purpose, the periodic boundary conditions are obtained to advance in phase by

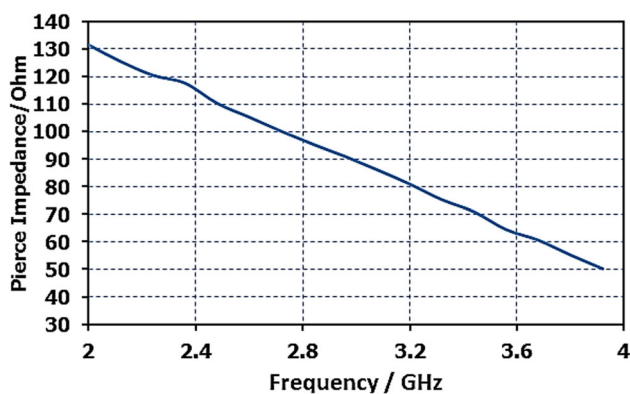


Fig. 7 Pierce impedance of the WRH

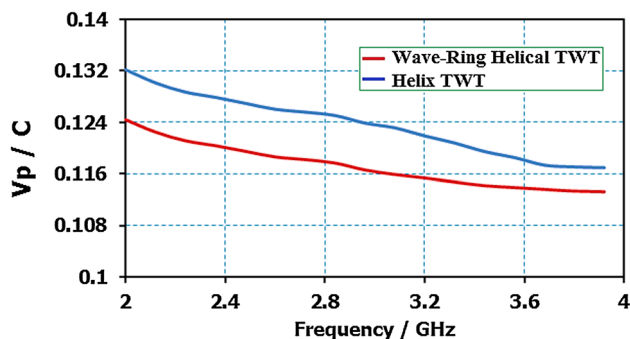


Fig. 8 The dispersion diagram based on phase velocity versus frequency

sweeping the parameters in CST MWS. The sweep parameter gives the interaction impedance and phase velocity directly in terms of frequency. In Fig. 7, the Pierce impedance values are shown as a function of frequency for the slow-wave structure operation.

The RF wave phase velocity must reach the electron beam velocity to proper the impedance matching. Figure 8 shows the normalized phase velocity as a function of the frequency in the cold test for WRH and conventional helix. It is clear that the phase velocity decreases with increasing of the frequency. The phase velocity of the WRH is smaller than the conventional helix.

Hot test simulation results

To show the amplification of the RF wave, the simulation of the hot test is carried out with CST-PS software. The simulated geometry of the TWT with WRH for hot test analysis is shown in Fig. 9. As seen in this figure, the charged particles leave the electron gun and are entered in the WRH. The electron beam is focused by a permanent magnet (PPM) structure [18].

Figure 10 shows the output power as a function of the input power for WRH-TWT at 3 GHz frequency. As seen in this figure, the output power increases linearly until

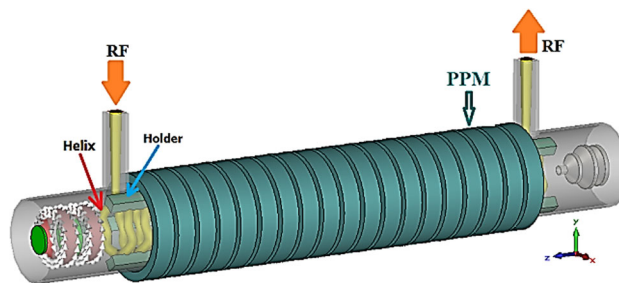


Fig. 9 The perspective view of WRH-TWT structure

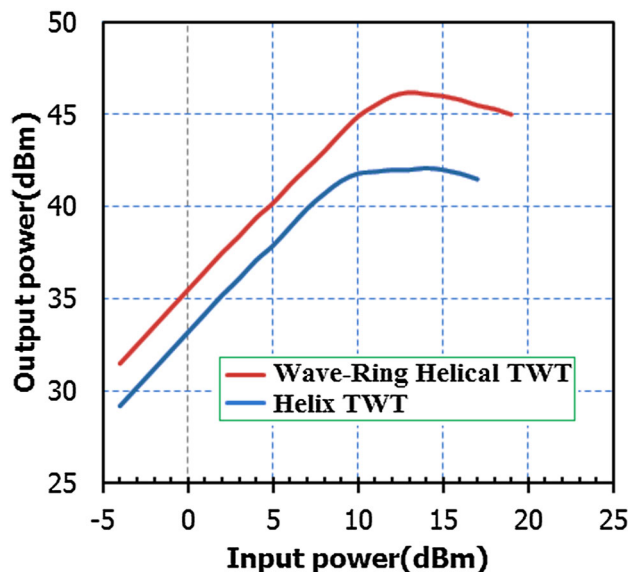


Fig. 10 Transfer characteristics of the wave-ring helical TWT at a frequency of 3 GHz

saturation has occurred. To further amplify the input signal, more energy is transferred from the electron beam to RF wave, and the speed of the electrons is reduced. If the input power increases after saturation point the output power is reduced. This is because of the nonlinear effects. In addition, Fig. 10 shows that if the input power is 19.95 mW at 3 GHz, then the output power produced will be 41.69 W. In such a situation, according to Fig. 12, the saturation gain is 27 dB. As seen in this figure, the output power for WRH is greater than the conventional helix.

Figure 11 shows the saturated output power as a function of frequency. The simulation result illustrates that the saturated output power for WRH-TWT occurs from 2.6 to 3.2 GHz.

As seen in Fig. 12, the TWT based on WRH structure can deliver a maximum gain of 28 dB at 2.84 GHz. As apparent in Figs. 11 and 12, in the frequency range 2–4 GHz the output power and gain are greater than conventional helix.

In this paper, the geometric dimensions of WRH are designed 80% smaller than the previous SWS structure,

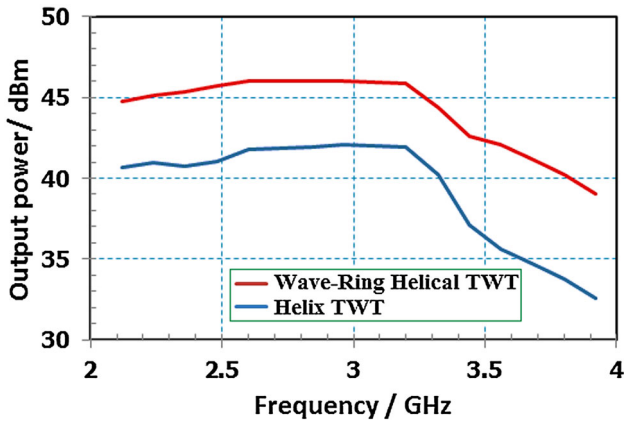


Fig. 11 Saturated output power of the S-band WRH-TWT as functions of the frequency

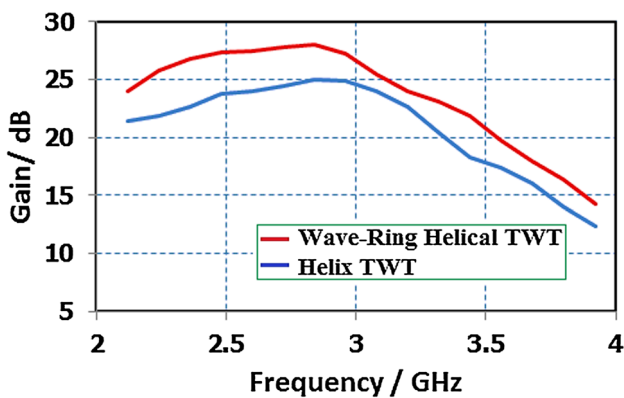


Fig. 12 Saturated gain of the S-band WRH-TWT as functions of the frequency

Table 3 Characteristics of electron beam

Parameter	Specification
Source type	Circular
Particle type	Electron
Emission model	Fixed
Beam voltage	3 kV
Beam current	50 mA

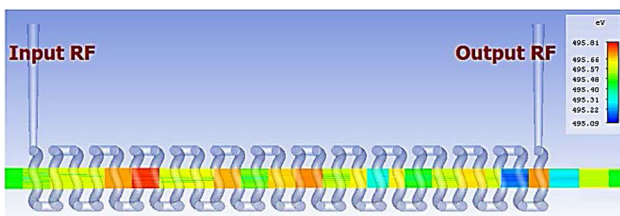


Fig. 13 Particle trajectory inside the WRH-TWT. It shows bunching of electrons due to WRH structure inside

Table 4 Design parameters of the WRH-TWTA

Parameter	Specification
Bandwidth	2–4 GHz
Saturated output power	39.8 W
Saturated gain	28 dB
Cathode voltage	–3 kV
Anode voltage	+0.1 kV
Focusing magnetic field	1.5 T
Tube length	100.50 mm

which makes it possible to reduce simulation time and further state investigation, and do further evaluation of the structure of WRH. On the other hand, we explore small-scale structures and its efficiency, simultaneously. Table 3 shows the profile of the electron beam in the WRH structure. The radius of the cathode determines the radius of the electron beam, which is chosen to be usually half the radius of the inner helix [19].

The beam–wave coupling of the designed TWT using the WRH structure is shown in Fig. 13. It shows the bunching of electrons inside the WRH structure. The coupled energy ramp along the longitudinal direction shows the modulation of the electrons due to the interaction with the WRH. The design parameters based on PIC CST simulations are shown in Table 4.

Conclusion

In this paper, the new slow-wave structure WRH in the S-band frequency range is analyzed using the CST-PS software. In this frequency range, the structure shows good performance. The hot and cold test results confirm it. The comparison with conventional helix is investigated. The most interesting result of this work is increasing the length of the path of the RF wave at WRH structure without increasing the size of the geometry of SWS, which has industrial and technological importance. Simulation results on WRH-TWT show the saturated output power of 39.8 W at 2.6–3.2 GHz, corresponding to a saturated gain of 28 dB. In the selected frequency range, the output power and gain are greater than conventional helix.

Open Access This article is distributed under the terms of the Creative Commons Attribution 4.0 International License (<http://creativecommons.org/licenses/by/4.0/>), which permits unrestricted use, distribution, and reproduction in any medium, provided you give appropriate credit to the original author(s) and the source, provide a link to the Creative Commons license, and indicate if changes were made.

References

1. Kompfner, R.: The invention of the traveling-wave tube. *IEEE Trans. Electron. Dev.* **23**(7), 730–738 (1976)
2. Gilmour Jr., A.S.: “Traveling Wave Tubes”, in *Klystrons, Traveling Wave Tubes, Magnetrons, Cross-Field Amplifiers, and Gyrotrons*. Artech House, Norwood (2011)
3. Sensiper, S.: Electromagnetic wave propagation on helical structures (a review and survey of recent progress). *Proc. IRE* **43**(2), 149–161 (1955)
4. Birdsall, C.K., Everhart, T.E.: Modified contra-wound helix circuits for high-power traveling-wave tubes. *IRE Trans. Electron. Dev.* **3**(4), 190–204 (1956)
5. Sauseng, O.: Ring-bar slow-wave structures for wideband high power TWTs in the millimeter wave range. In: *IEDM Tech. Dig.*, pp. 1–22 (1982)
6. Liu, S.: Calculation of the parameters for ring-loop traveling wave tube in MMW. *Int. J. Infr. Millim. Waves* **21**(7), 1097–1101 (2000)
7. Döhler, G., Gagne, D., Gallagher, D., Moats, R.: Serpentine waveguide TWT. In: *IEDM Tech. Dig.*, pp. 485–488 (1987)
8. Zuboraj, M., Apaydin, N., Sertel, K., Volakis, J.L.: Half-ring helical structure for traveling wave tube amplifiers. *IEEE Trans. Plasma Sci.* **42**(11), 3465–3470 (2014)
9. Dyson, D.R., Clark, M.J., Smith, V.H.: Numerical analysis of ring-loop and ringbar slow wave structures for traveling wave tubes. In: *Transactions of IEEE international vacuum electronics conference*, pp. 46–47 (2003)
10. LeBorgne, R.H., et al.: Development of an 800 W, Ka-band, ring-bar TWT. In: *Technical digest, IEDM* (1990)
11. Cain, W.N., Grow, R.W.: The effects of dielectric and metal loading on the dispersion characteristics for contrawound helix circuits used in high-power traveling-wave tubes. *IEEE Trans. Elec. Dev.* **37**(6), 1566–1578 (1990)
12. Birdsall, C.K., Everhart, T.E.: Modified contrawound helix circuits for high-power travelingwavetubes. *Hughes Aircraft Company, Tech. Memo.* 400 (1955)
13. Watkins, D.A.: *Topics in Electromagnetic Theory*, vol. 2. Wiley, New York (1958)
14. Sensiper, S.: Electromagnetic wave propagation on helical structures. *Proc. IRE* **43**, 149 (1955)
15. Uhm, H.S., Choe, J.Y.: Electromagnetic wave propagation in a conducting waveguide loaded with a tape helix. *IEEE Trans. Microwave Theory Tech.* **31**, 704 (1983)
16. Jung, A.R.: 10 kW and up, from a helix TWT? In: *Technical digest, IEDM*, pp. 530–553 (1978)
17. Gittins, J.F.: *Power Traveling Wave Tubes*. Elsevier, New York (1965)
18. Baird, M.: *mPPM program manual user’s guide* (2002)
19. Shiffer, D., Nation, J.A., Wharton, C.B.: High-power traveling-wave tube amplifier. *Appl. Phys. Lett.* **54**(7), 674–677 (1989)

Publisher’s Note

Springer Nature remains neutral with regard to jurisdictional claims in published maps and institutional affiliations.